Scanning Microscopy

Volume 9 | Number 3 Article 20

9-6-1995

# Comparison of DNA Fragmentation and Color Thresholding for Objective Quantitation of Apoptotic Cells

D. R. Plymale
*Tulane University*

D. S. Ng Tang
*Baylor College of Medicine*

C. D. Fermin
*Tulane University*

D. E. Lewis
*Baylor College of Medicine*

D. S. Martin
*Tulane University*

*See next page for additional authors*

# Comparison of DNA Fragmentation and Color Thresholding for Objective Quantitation of Apoptotic Cells


## Authors

D. R. Plymale, D. S. Ng Tang, C. D. Fermin, D. E. Lewis, D. S. Martin, and R. F. Garry

Scanning Microscopy, Vol. 9, No. 3, 1995 (Pages 833-842) 0891-7035/94$5.00+.25
Scanning Microscopy International, Chicago (AMF O'Hare), IL 60666 USA

# COMPARISON OF DNA FRAGMENTATION AND COLOR THRESHOLDING FOR OBJECTIVE QUANTITATION OF APOPTOTIC CELLS

D.R. Plymale[1], D.S. Ng Tang[4], C.D. Fermin[1,2], D.E. Lewis[4], D.S. Martin[2], and R.F. Garry[1,3,*]

[1]Molecular and Cellular Biology Program, [2]Department of Pathology & Laboratory Medicine,
[3]Department of Microbiology and Immunology, Tulane University School of Medicine, New Orleans, LA
[4]Department of Microbiology and Immunology, Baylor College of Medicine, Houston, TX

(Received for publication May 11, 1995, and in revised form September 6, 1995)

## Abstract

Apoptosis is a process of cell death characterized by distinctive morphological changes and fragmentation of cellular DNA. Using video imaging and color thresholding techniques, we objectively quantitated the number of cultured CD4+ T-lymphoblastoid cells (HUT78 cells, RH9 subclone) displaying morphological signs of apoptosis before and after exposure to γ-irradiation. The numbers of apoptotic cells measured by objective video imaging techniques were compared to numbers of apoptotic cells measured in the same samples by sensitive apoptotic assays that quantitate DNA fragmentation. DNA fragmentation assays gave consistently higher values compared with the video imaging assays that measured morphological changes associated with apoptosis. These results suggest that substantial DNA fragmentation can precede or occur in the absence of the morphological changes which are associated with apoptosis in γ-irradiated RH9 cells.

**Key Words:** Apoptosis, γ-irradiation, human-immunodeficiency virus, color thresholding, DNA fragmentation.

*Address for correspondence and present address:
Robert F. Garry
Department of Microbiology and Immunology,
Tulane University School of Medicine,
1430 Tulane Avenue, SL-38,
New Orleans, LA 70112-2699
USA

Telephone number: (504) 587-2027
FAX number: (504) 588-5144
E-Mail: rgarry@tmcpop.tmc.tulane.edu

## Introduction

Apoptosis is a process of cell death characterized by distinctive morphological changes that include condensation of nuclear material and fragmentation of the cell into discrete membrane enclosed structures (Kerr *et al.*, 1972; Williams, 1991; Hoffman and Liebermann, 1994; Lewis *et al.*, 1994; McCloskey *et al.*, 1994; Ohno *et al.*, 1994). Apoptosis can be distinguished on morphological and physiological criteria from other forms of cell death, such as necrosis (Allan and Harmon, 1986). Another important feature of apoptotic cell death is fragmentation of cellular DNA at regular, 200 base pair (bp) intervals as a result of internucleosomal cleavage by a $Ca^{++}$ activated endonuclease (Collins *et al.*, 1992; Lewis *et al.*, 1994). Apoptosis is a biologically important mechanism by which unwanted cells are removed, and is instrumental during development and refinement of organ formation (Finlay *et al.*, 1982; Humbert *et al.*, 1991; Cohen *et al.*, 1992; Hamburger, 1992; Braccilaudiero *et al.*, 1993; Estus *et al.*, 1994; Hoffman and Liebermann, 1994; Hyde and Durham, 1994; Kelley *et al.*, 1994; Yin *et al.*, 1994; Lassmann *et al.*, 1995). For example, redundant synaptic contacts are removed by apoptotic cell death (Finlay *et al.*, 1982; Sengelaub and Finlay, 1982; Ard and Morest, 1984; Oppenheim, 1984, 1991; Hamburger, 1992; Johnson and Deckwerth, 1993). Apoptosis is also thought to be critically important during development of the immunological repertoire, and appears to be the way that T-cells are eliminated in the thymic environment (Murphy *et al.*, 1990; Green and Cottler, 1992). In this case, activation of thymic cells by exposure to self antigens leads to death by apoptosis. Apoptosis also occurs in response to a variety of stimuli including: hormone deprivation, mild thermal and metabolic stress, cell killing by cytotoxic T-lymphocytes and Natural Killer cells, and chemotherapy (Sellins and Cohen, 1991; Cohen, 1992; Day *et al.*, 1994; Ziv *et al.*, 1994; Smyth and Trapani, 1995). A number of viruses, including human immunodeficiency virus (HIV), the etiologic agent of acquired immune deficiency syndrome (AIDS), have been reported to

induce cell death via apoptotic pathways (Laurent-Crawford *et al.*, 1991; Terai *et al.*, 1991; Gougeon *et al.*, 1993; Lewis *et al.*, 1994; Lu *et al.*, 1994).

Substantial variation has been reported using different methods for the quantification of apoptosis, even in cases where similar cells or inducers of apoptosis have been utilized. For example, some laboratories have reported high rates of apoptotic cell death during acute infection of CD4+ T-lymphoblastoid cells by HIV *in vitro* (Laurent-Crawford *et al.*, 1991; Terai *et al.*, 1991), whereas other investigators have found that the number of cells dying by apoptosis represents only a minor population of the cells killed by HIV during acute infection *in vitro* (Bergeron and Sodroski, 1992; Plymale *et al.*, unpublished observations). Discrepancies between various laboratories may result from variations in techniques used or inherent difficulties in quantifying morphological changes or DNA cleavage products. For example, it is often difficult to distinguish apoptotic cells from late stage necrotic cells by DNA based assays (Compton, 1992; Zamai *et al.*, 1993; Bryson *et al.*, 1994). Likewise, some assays that measure fragmentation of DNA into multimers of 180-200 base pairs on agarose gels may not be sensitive enough to accurately quantitate a low percentage of cells undergoing apoptosis (Plymale *et al.*, unpublished observations). Moreover, we have noted, and others have suggested that DNA fragmentation may not always correlate with the morphological changes associated with apoptosis (Oberhammer *et al.*, 1993; Omerod *et al.*, 1993). It is important to consider that there may be mechanisms leading to DNA fragmentation that do not result in the morphological changes characteristic of apoptosis. For example, one potential source of fragmented DNA is cellular debris (Zamai *et al.*, 1993). This may be especially relevant in cell culture systems such as RH9 cells that achieve high cell densities. Cells that exhibit fragmented DNA and/or chromatin condensation in response to variables other than those intended for analysis may also affect quantitative results. Factors such as sample handling, the nature of the cell line, cell densities, kinetics of cell growth, temperature, or low level irradiation from extraneous sources must also be evaluated and carefully controlled.

Video imaging technologies such as color thresholding offer methods for objective quantitation of morphological data that have not yet been evaluated for measuring apoptosis (Fermin *et al.*, 1992; Fermin and Degraw, 1995). In this study, color thresholding was used to distinguish the chromatin of apoptotic cells from that of non-apoptotic and mitotic cells. Color thresholding is able to separate adjacent pixels based on the saturation of each color, rather than density. This property allows separation of pixels containing apoptotic chromatin from non-apoptotic condensed chromatin apparent during mitosis. This technology is able to quantitate the number of cells in a culture with extensive condensation of nuclei that is characteristic of apoptotic cells. The results show that color thresholding is better able to separate closely related hues than monochrome thresholding. We compared the results of this assay with a sensitive and quantifiable assay for measuring DNA fragmentation previously developed by some of us (Lewis *et al.*, 1994). In comparing results obtained using these objective assays, we observed that substantial DNA fragmentation can precede or occur in the absence of the morphological changes associated with apoptosis in $\gamma$-irradiated cells of an established CD4+ T-lymphoblastoid cell line.

## Material and Methods

### Cell cultures

Cells from the RH9 subclone of the CD4+ cutaneous human T-lymphoma cell line HUT-78 were propagated in RPMI 1640 tissue culture medium supplemented with 10% Serum Plus (JRH Biosciences) and 1% penicillin/streptomycin in a 37°C incubator (Rasheed *et al.*, 1986). The cells were grown in tightly sealed flasks (75 $mm^2$) to maintain $CO_2$ levels. Human immuno-deficiency virus type 1 (HIV-1) strain HTLV-IIIB (also known as LAI), kindly provided by the Laboratory of Tumor Cell Biology at NIH, was propagated in RH9 cells, and virus stocks were prepared from chronically-infected RH9 cells. Stocks were stored at -98°C. Chronically HIV-infected cultures represent cells that have survived the acute cytopathic effects of HIV after infection at a multiplicity of approximately 10 infectious units per cell. Apoptosis was induced in uninfected RH9 cells by exposing them to 600 rads $\gamma$-radiation from a $^{137}Ce$ source. Cells were cultured overnight, and DNA was then extracted or the cells were prepared for microscopy.

### Quantitation of fragmented DNA by end-labeling

End labeling of the DNA fragments greatly enhances the sensitivity of the agarose gel DNA fragmentation assay for apoptotic cells and enables accurate objective quantification of apoptosis in lymphocytes from AIDS patients (Lewis *et al.*, 1994). The performance of this assay compares well with often used single cell flow cytometric assays (Lewis *et al.*, 1994). Using end-labeling it is possible to detect DNA ladders in PBMC from AIDS patients even though only a few percent of cells may be apoptotic by morphological criteria (Lewis *et al.*, 1994). This objective technique was utilized in the current study and compared to an objective morphometric technique for quantitation of apoptosis described below. Briefly, DNA was extracted from pelleted cells by

digestion for one hour in buffer consisting of 50 mM Tris, 10 mM ethylenediaminetetraacetic acid (EDTA), 0.5% sodium dodesyl-sulfate (SDS), and 0.5 mg/ml freshly added proteinase K (pH 8). The lysates were then pelleted and treated with 0.5 mg/ml RNAse A in Tris EDTA buffer for one hour. The lysates were stored at 4°C overnight, then electrophoresed on agarose gels. Southern blotting was performed with $^{32}$P-labeled genomic human DNA extracted from U937 cells, a human monocyte line. This DNA, 75 ng, was labeled with [$\alpha$-$^{32}$P]dCTP by T4 DNA polymerase using a Pharmacia oligolabeling kit (Pharmacia, Milwaukee, WI). This is a standard procedure that results in a comparable labeling efficiency of DNA molecules present in a complex mixture. The labeled probe was purified with Nick columns (Pharmacia). Quantitation was performed by counting on a Betagen Betascope 603 Blot Analyzer (Betagen Corp., Waltham, MA). This instrument detects radioactivity over a wide linear range, making quantitation more accurate than methods using film. The total number of counts is divided into the number of counts in the bottom 85 to 90% of the gel, including DNA below 23,130 bp.

### Microscopy with quantitative video-image analysis

To quantify apoptosis by morphometric techniques, cells were pelleted, fixed in 2% paraformaldehyde and 2% glutaraldehyde in phosphate buffer (pH 7.4), and post-fixed in 1% osmium tetroxide. Pellets were then embedded in LX112 epoxy, sectioned at 70 nm, and stained with uranyl acetate and lead citrate in a LKB autostainer. Images were recorded with a Zeiss 109 transmission electron microscope at magnifications of 10,000-100,000X, on Kodak emulsion 6415 (120 mm). One to two $\mu$m thick sections were stained with toluidine blue and phenylenediamine (Fermin and Igarashi, 1984), placed on an Olympus BH2 microscope and viewed at 1,500X magnification directly on the video screen of a V150® imaging system from Oncor (Gaithersburg, MD). This system separates primary and secondary colors based on their hue-saturation-intensity (HSI), theoretically allowing 16 million color possibilities. We used color thresholding rather than monochrome thresholding, because differences between adjacent pixels are not always easy to separate with monochrome systems since these often can not separate hues of similar intensities (e.g., a dark brown and dark blue). This is particularly important when trying to count particles (gold isotopes) from dark backgrounds (e.g., dark field and *in situ* hybridization). The HSI mode is based on the same principle that the human brain uses to distinguish colors. HSI consists of a three dimensional space within which discrimination of colors is performed without the need of filter selection (Fermin and Degraw, 1995, Fermin *et al.*, 1992). This is important because filters only select for hue, not for saturation, and the systems that rely on filters are usually slow and expensive. An apoptotic cell is identified by the user, and the condensed chromatin pixel saturation (color threshold) is stored in memory. Then, the slide is scanned in real time and whenever the system encounters the stored value, the pixels above that threshold are indicated. The total number of pixels within the threshold are counted, or the cross-sectional area of the chromatin identified by the computer is calculated and cells counted (Fermin *et al.*, 1992; Fermin and Degraw, 1995).

## Results

Figures 1 to 4 are black and white representations of the toluidine blue/phenylenediamine color stain we used to separate apoptotic chromatin from mitotic and interphase chromatin. A pixel-pixel amplification of chromatin boxed-in Figure 5 shows in Figures 6 and 7 that slight variations in blue hue were separated. The narrow difference among blue pixels is effortlessly separated with color thresholding (Figure 7). Once the apoptotic chromatin is within threshold, it can be binarized and objects can be subjected to morphometric manipulations (Figure 8). Monochrome thresholding can also be used for separating various chromatin conformations (Figures 9 and 10). However, the ability to separate objects of closely related densities such as apoptotic chromatin and cytoplasmic inclusions (Figure 11) is often difficult (Figure 12).

During logarithmic growth, cells from cultures of RH9 cells, a human T-lymphoblastoid cell line, exhibit a low spontaneous rate of apoptosis as measured by morphological techniques. However, apoptotic cells are observed in cultures that have survived the acute cytopathic effects of HIV and established HIV persistently-infected cultures (Figures 1 to 4). Certain of these HIV chronically-infected cells display the signature morphology of apoptosis with condensed chromatin and nuclear membrane-bound dense bodies (Figures 1, 4, 9, 10, 11). These nuclear membrane-bound dense bodies may also appear to bleb into the cytoplasm as the cell continues on its pathway of death (Figures 11 and 12). Breakdown of the cell with release of nuclei with condensed chromatin is also observed in these chronically-infected cultures (Figure 3). Other cells in these chronically-infected cultures do not appear to be apoptotic, but show evidence of vacuolar degeneration (Figures 2 and 4), a hallmark of the acute cytopathic effects of HIV (Fermin and Garry, 1992). Uninfected RH9 cells contain dense cytoplasmic granules and, occasionally, mitotic chromatin which confound the quantitation of apoptotic cells (Figure 5 and 10). To accurately quantitate

the number of apoptotic cells in a population, it is necessary to distinguish the dense cytoplasmic granules and mitotically condensed chromatin from apoptotic chromatin condensation. Our observations suggest that this can be achieved using color thresholding (insets Figure 1, and Figures 5 to 8). The condensed nuclei of apoptotic HIV-infected RH9 cells had consistently different thresholds than normal cellular components (compare cells with arrows in Figures 5 and 6). Such separation allows apoptotic cells to be identified with color thresholding. Mitotic chromatin also has different thresholds from apoptotic chromatin, allowing these cells to be discerned by this method. While we have found that thresholding methods for quantitating apoptotic cells have the greatest utility for analyses conducted at the light microscopic level, these video imaging techniques are also useful at the ultrastructural level. For example, it can be demonstrated in black and white electron micrographs that the nuclear membrane bound bodies of apoptotic cells contain highly condensed chromatin (Figure 11). Electron-dense bodies from a monochrome source, such as an EM negative, have similar densities as nuclear chromatin and could have thresholds similar to that of the chromatin in a monochrome mode (Figures 11 and 12), but different thresholds in a color mode (Figures 5 to 8).

Previously, we described a method for assessing DNA fragmentation on agarose gels that employs probing with $^{32}$P-labelled genomic DNA and quantitation on a Betascope (Lewis *et al.*, 1994). The goal of the current study was to compare video imaged morphology and quantitative DNA fragmentation, two objective assays for measuring apoptotic changes. Logarithmically growing RH9 cells that display a low rate of spontaneous apoptosis were exposed to 600 rads of $\gamma$-irradiation to induce apoptosis. As expected, the numbers of untreated RH9 cells with condensed nuclei and other morphological changes characteristic of apoptosis was consistently low. Fewer than 1% of cells were apoptotic as determined by objective morphological criteria. The percentage of apoptotic cells measured by color thresholding increased to 9.7% after exposure to $\gamma$-irradiation. By comparison, the amount of DNA fragmentation in these cell cultures, either before or after $\gamma$-irradiation, was consistently higher than the number of cells displaying morphological signs of apoptosis (Figure 13).

## Discussion

A variety of environmental or physiological stimuli can activate or trigger the cellular machinery for apoptosis (Murphy *et al.*, 1990; Williams, 1991; Cohen, 1992; Motyka *et al.*, 1993; Day *et al.*, 1994; Lewis *et al.*, 1994; Ziv *et al.*, 1994). Techniques for quantifying apoptosis by assessing DNA fragmentation on agarose gels can be made objective by $^{32}$P-probing of the cleaved DNA and quantitation on a Betascope (Lewis *et al.*, 1994). Our current results suggest that color thresholding also permits objective quantitation of apoptotic cells in a given population by morphological methods. Furthermore, color thresholding permits cells to be recounted since a permanent record exists in the slides, and the morphology of cells can be double-checked by independent observers. Both of these methods for quantifying apoptosis have the advantage of eliminating observer bias. Exposure to $\gamma$-irradiation results in a large population of cells in the $G_2$ phase of the cell cycle and in the induction of apoptosis (Bryson *et al.*, 1994). In RH9 cells exposed to $\gamma$-irradiation, we observed a higher percentage of DNA fragmentation than of cells displaying apoptotic morphology. These results suggest that substantial DNA fragmentation occurs in the absence of detectable nuclear condensation and other characteristic morphological changes in these $\gamma$-irradiated CD4+ T-lymphoblastoid cells. Our results also contribute to the concept that there are multiple distinct path-

**Figure 1.** Low magnification of persistently infected RH9 cells. Several multinucleated cells (M), apoptotic cells (large arrows), a mitosing cell (arrowheads) and cellular debris (D) are shown. **Insert left:** Thresholds for the apoptotic chromatin shown at the arrowhead are red-cyan 97-125, yellow-blue 145-202 and luma 6-90. **Insert right:** Using these thresholds only the pixels representing the chromatin of the apoptotic cells are chosen, shown here in black and white (arrowheads). A color representation of a similar preparation is shown in Figures 5-8.

**Figure 2.** Non-apoptotic RH9 cell with many HIV virions attached (arrow). The cells display typical vacuolization (V), slightly heterochromatic nucleus (N) and several osmiophilic granules that could represent lysosomes. Mitochondria (M) are swollen.

**Figure 3.** A nucleus surrounded by cellular debris and HIV particles (arrow). The nuclear membrane (N) is attached and the perichromatin is still in place. Condensed chromatin (CCH) is clearly distinguishable from non-condensed chromatin (NCH), but it is impossible to determine if the DNA of the chromatin is fragmented or not by electron microscopy. At the light microscopy level, distinction between chromatin from whole cells and that of disintegrating cells can easily be made.

**Figure 4.** Section through portion of the cytosol and nuclear condense chromatin of an apoptotic cell. The chromatin (arrows) is clearly distinguishable from the cytoplasmic organelles, including mitochondria (M) and vacuoles (V).

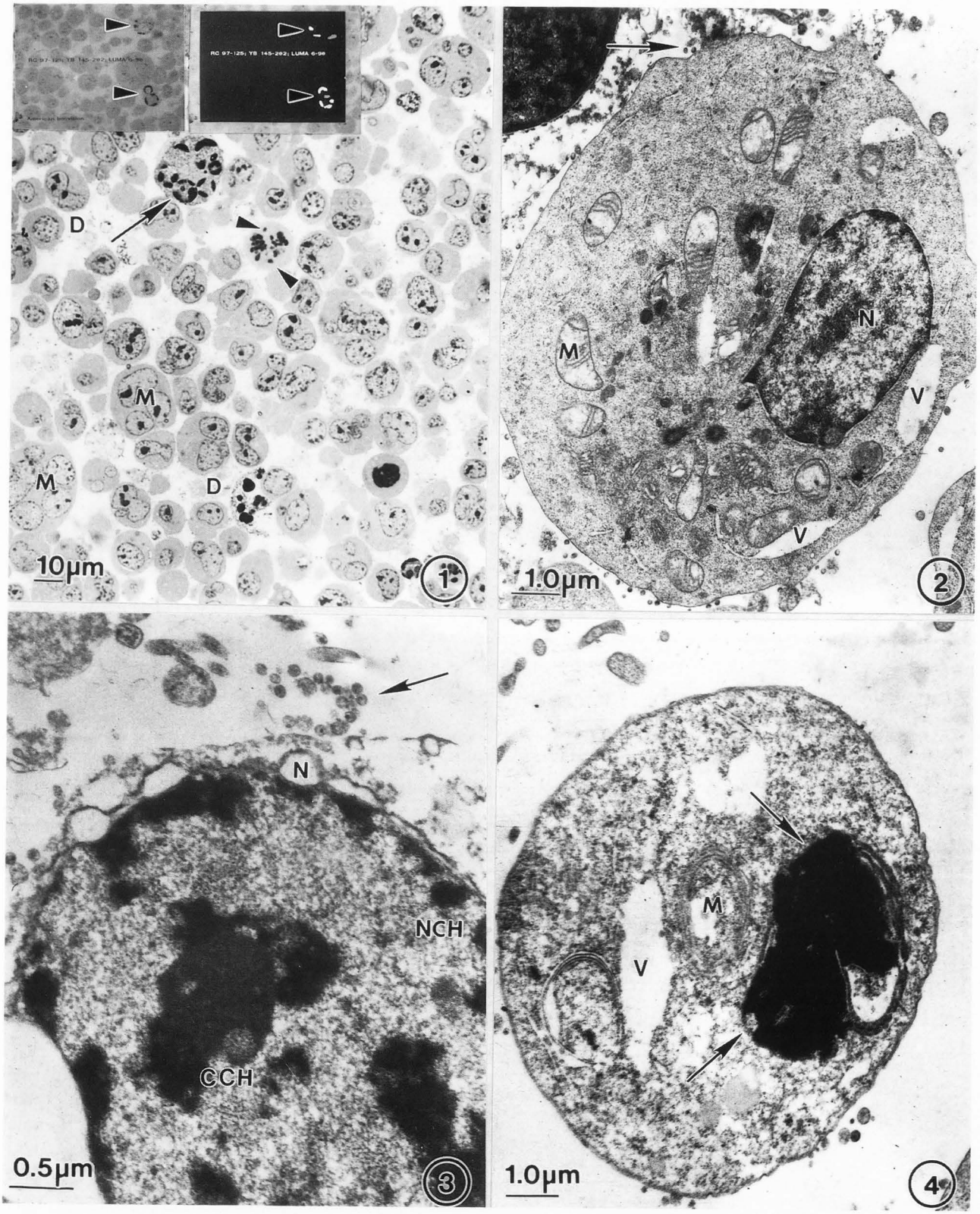
D
M
M
D
10μm
1
N
M
V
V
1.0μm
2
N
NCH
CCH
0.5μm
3
M
V
1.0μm
4

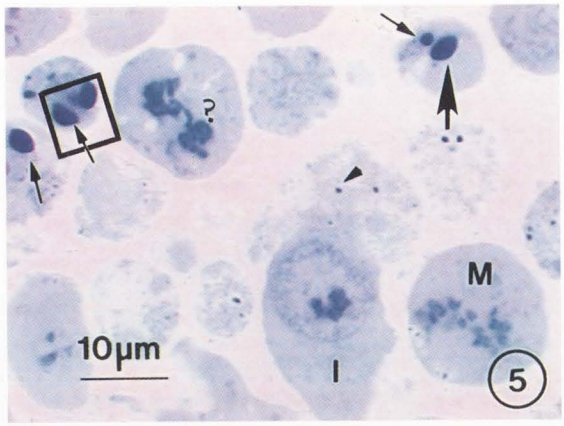
?
M
I
10μm
5

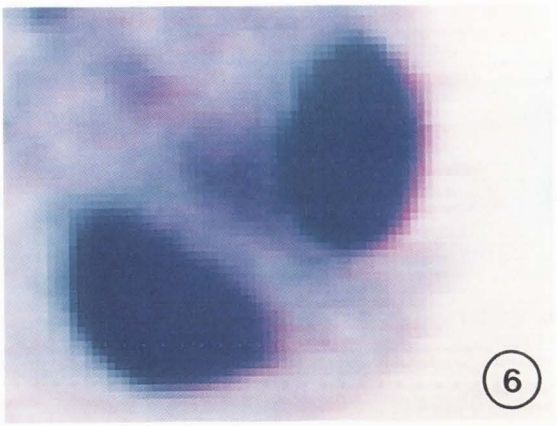
6

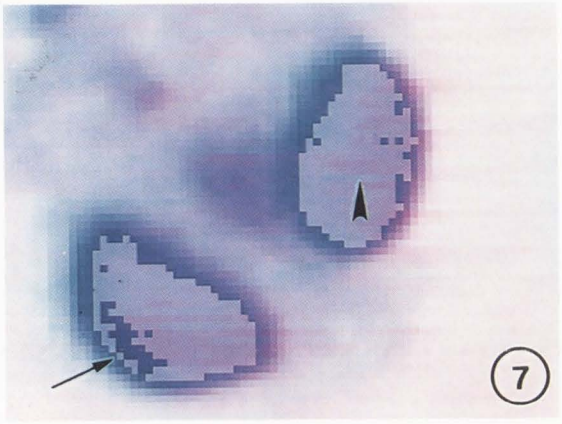
7

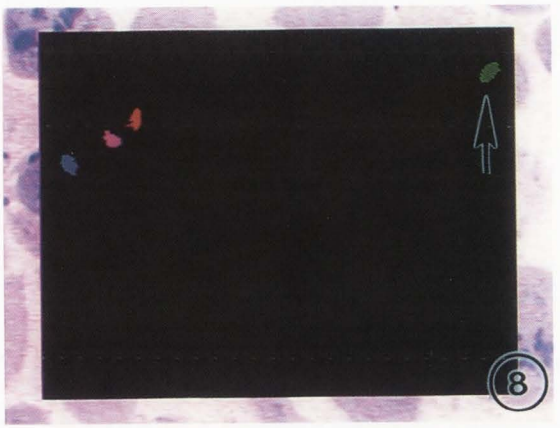
8

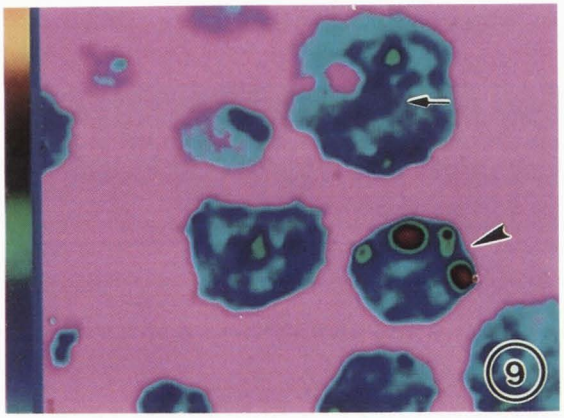
9

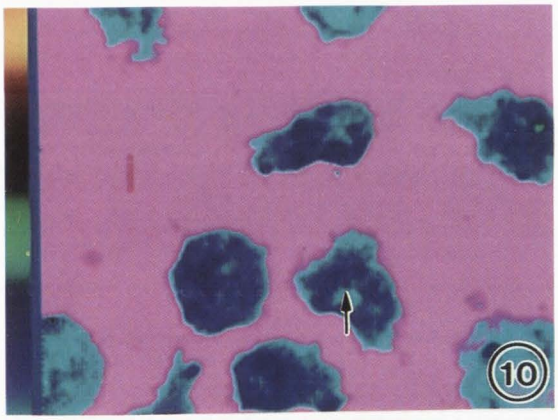
10

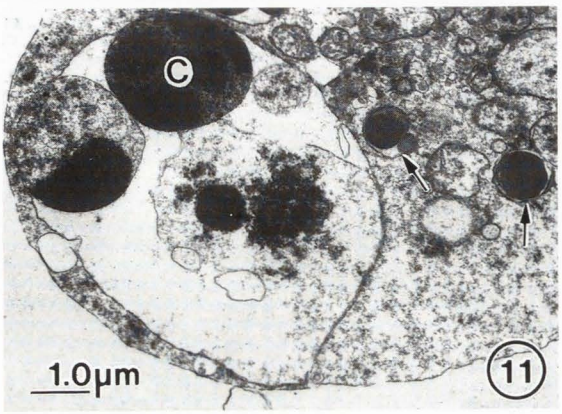
C
1.0μm
11

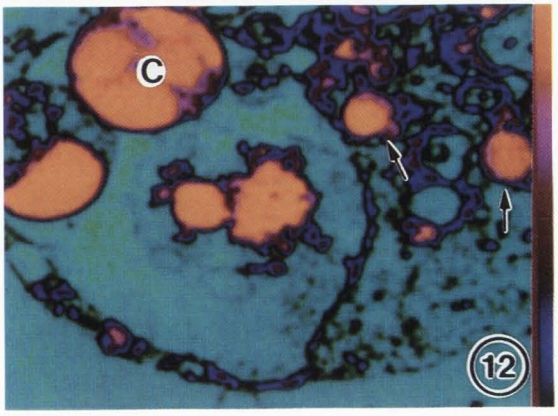
C
12

**Figure 5.** True-color image of a 1.5 $\mu$m thick plastic section stained with toluidine blue and paraphenylenediamine. Apoptotic nuclei (small arrows), mitotic nuclei (M) and interphase nuclei (I) are shown. In addition, condensed chromatin at an intermediate undefined stage (?) is illustrated. Note that the density of the extranuclear inclusions (arrowhead) and the apoptotic chromatin (large arrow) is similar and both appear dark blue.

**Figure 6.** When the individual pixels (at 24 bits resolution) of the apoptotic nuclei in the box of Figure 5 are visualized with a "zoom" function of the system, it is clear that not every pixel has the same saturation. This level of magnification permits choosing individual pixels during thresholding.

**Figure 7.** Same frame as Figure 6, after applying color thresholding. Choosing color thresholding by pointing to individual pixels (arrowhead), and based on the saturation of those pixels' color rather than the monochrome intensity, permits separating them from other blue pixels. This is possible even when the color (hue) is the same, because those pixels not chosen (arrow) have different saturation values.

**Figure 8.** The narrow separation of pixel saturation from 16 million color possibilities permits a very specific identification of structures within a chosen threshold. On this binarized image of Figure 5 with objects that have similar color thresholds, it is clearly seen that of the chromatin indicated by arrows in Figure 5, only the true apoptotic chromatin was chosen (blue, red and green objects). The questionable chromatin illustrated on Figure 1 by (?), the interface chromatin by (I), the mitotic chromatin by (M) and the extranuclear dense bodies (arrow) were not chosen, even though the upper and lower size limits chosen would have included those objects. This specific isolation of objects is not possible with monochrome thresholding which is illustrated in Figures 9-12 below.

**Figure 9.** Objects with similar hues but of closely related densities are separated from each other when the pixel spread among them is wide enough to add pseudo-color from prechosen look-up tables. An infected RH9 cell, viewed under identical magnification as Figure 5, thresholded in a monochrome imaging mode, and to which pseudocolor was added, illustrates that separation of apoptotic chromatin (arrowhead) can be made from the normal condensed chromatin (arrow) found at interphase. However, the levels of separation possible with a monochromatic system is limited by the range of values on the look up table used to generate the false colors. Color thresholding can theoretically separate 16 million differences.

**Figure 10.** Uninfected cells viewed under identical magnification as Figure 5, subjected to the same threshold as shown in Figure 9, showing that the chromatin of non-apoptotic cells is not selected and remains outside the chosen threshold. Unfortunately, monochrome thresholding cannot always separate such closely related intensities.

**Figure 11.** The best illustration of the limitation that monochrome imaging mode has in separating hues of closely related densities is the digitization of black and white negatives from the electron microscope (image source is monochrome). The electron density of the condensed chromatin and of the extranuclear dense bodies is too close for the chosen lookup table to separate them. Figures 5-8 illustrate that such separation is readily accomplished with color thresholding. Electron micrograph of an apoptotic HIV-persistently infected RH9 cell. Electron density, and hence, intensity of the dark objects is difficult to separate among objects. Condensed chromatin (C) inside what is left of the nucleus appears similar to membrane bound vesicles (arrows) in the cytoplasm.

**Figure 12.** Same cell as in Figure 11 after gray-scaling and assignment of false color. Note that the cytoplasmic bodies (arrows) have the same intensity as the nuclear chromatin but are not confined by the nuclear membrane. When the image is digitized in a monochrome mode and the scheme utilized for analysis of Figures 9-10 is applied, both the condensed chromatin in the nucleus and the vesicles are within threshold. In this case, monochromaticity is provided by the black and white negative of the electron microscope, but the unwanted consequence of monochromaticity is the same, namely that the number of possible differences that can be separated between adjacent pixels is limited.

---

ways or programs that may result in cell death. The morphological features of apoptosis have previously been dissociated from the appearance of DNA laddering in thymocytes (Cohen *et al.*, 1992). In other cases, endonuclease activation may occur in the late stages of the apoptotic program leading to a different relation between DNA fragmentation and apoptotic morphology than observed in our studies (Omerod *et al.*, 1993; Bryson *et al.*, 1994). DNA fragmentation may be absent or incomplete in apoptotic cells (Cohen *et al.*, 1992; Oberhammer *et al.*, 1993), but may also be present in late stage necrotic cells (Compton, 1992).

In future studies, it will be important to compare results in RH9 cells with other CD4+ lymphoblastoid cell lines and with cells from other lineages. Peripheral blood cells that are removed from the circulation and placed in culture die by apoptosis under certain culture conditions. Both CD4+ and CD8+ cells from AIDS

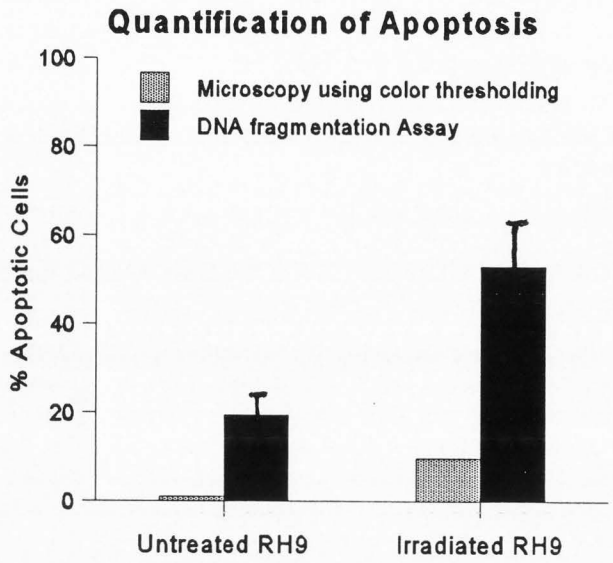


**Figure 13.** Quantification of apoptosis in γ-irradiated RH9 cells by objective techniques. Apoptosis was quantified before and after exposure to 600 rads γ-irradiation by assessing DNA fragmentation on agarose gels using a technique that probes DNA with $^{32}$P-labelled genomic DNA quantitation of counts on a Betascope (Lewis *et al.*, 1994), and by color thresholding methods. The percentage of fragmented DNA in untreated RH9 cells is 19 ± 5 as measured by the DNA fragmentation assay. Only 1 (5 of 483) percent of cells in this population display the morphological signs of apoptosis. Upon γ-irradiation, the percentage of DNA that is fragmented increases to 53 ± 11 and 9.7% (25 of 258) of these cells are apoptotic by morphological criteria.

---

patients display higher rates of apoptotic cell death when placed in culture than cells from uninfected individuals (Lewis *et al.*, 1994) or HIV-infected, asymptomatic individuals (Echaniz *et al.*, 1995). Therefore, it will also be important to compare results in primary cells with established cell lines.

Our results suggest that a comprehensive evaluation of apoptotic and other cell death pathways will require the application of multiple techniques that measure a variety of parameters.

## Acknowledgements

This work was supported by grants from the NIH to R.F. Garry (AI43754, DE10862) and D.E. Lewis (AI36211), and a grant from NASA (1516) to C.D. Fermin.

## References

Allan DJ, Harmon BV (1986) The morphologic categorization of cell death induced by mild hyperthermia and comparison with death induced by ionizing radiation and cytotoxic drugs. Scanning Electron Microsc **1986**; III: 1121-1133.

Ard MD, Morest DK (1984) Cell death during development of the cochlear and vestibular Ganglia of the chick. Int J Dev Neurosci **2**: 535-547.

Bergeron L, Sodroski J (1992) Dissociation of unintegrated viral DNA accumulation from single-cell lysis induced by human immunodeficiency virus type 1. J Virol **66**: 5777-5787.

Braccilaudiero L, Vigneti E, Iannicola C, Aloe L (1993) NGF retards apoptosis in chick embryo bursal cell *in vitro*. Differentiation **53**: 61-66.

Bryson GJ, Harmon BV, Collins RJ (1994) A flow cytometric study of cell death: Failure of some models to correlate with morphological assessment. Immunol Cell Biol **72**: 35-41.

Cohen JJ (1992) Glucocorticoid-induced apoptosis in the thymus. Semin Immunol **4**: 363-369.

Cohen GM, Sun XM, Snowden RT, Dinsdale D, Skilleter DN (1992) Key morphological features of apoptosis may occur in the absence of internucleosomal DNA fragmentation. Biochem J **286**: 331-334.

Collins RJ, Harmon BV, Gobé G, Kerr JFR (1992) Internucleosomal DNA cleavage should not be the sole criterion for identifying apoptosis. Int J Rad Biol **61**: 451-453.

Compton MM (1992) A biochemical hallmark of apoptosis: Intranucleosomal degradation of the genome. Cancer Metastasis Rev **11**: 105-119.

Day ML, Zhao X, Wu SX, Swanson PE, Humphrey PA (1994) Phorbol ester-induced apoptosis is accompanied by NGFI-α and c-fos activation in androgen-sensitive prostate cancer cells. Cell Growth Differ **5**: 735-741.

Echaniz P, Dolores de Juan M, Cuadrado M (1995) DNA staining changes associated with apoptosis and necrosis in blood lymphocytes of individuals with HIV infection. Cytometry **19**: 164-170.

Estus S, Zaks WJ, Freeman RS, Gruda M, Bravo R, Johnson EM (1994) Altered gene expression in neurons during programmed cell death: Identification of c-jun as necessary for neuronal apoptosis. J Cell Biol **127**: 1717-1727.

Fermin C, Degraw S (1995) Color thresholding in video imaging. J Anat **158**: 469-481.

Fermin CD, Garry RF (1992) Membrane alterations linked to early interactions of HIV with the cell surface. Virology **191**: 941-946.

Fermin CD, Igarashi M (1984) Dendritic growth

following labyrinthectomy in the squirrel monkey. Acta Otolaryngol (Stockh) **97**: 203-212.

Fermin CD, Gerber MA, Torre-Bueno J (1992) Colour thresholding & objective quantification in bioimaging. J Microsc **167**: 85-96.

Finlay BL, Berg AT, Sengelaub DR (1982) Cell death in the mammalian visual system during normal development: II. Superior colliculus. J Comp Neurol **204**: 318-324.

Gougeon ML, Laurent-Crawford AG, Hovanessian AG, Montagnier L (1993) Direct and indirect mechanisms mediating apoptosis during HIV infection: Contribution to *in vivo* CD4 T cell depletion. Semin Immunol **5**: 187-94.

Green DR, Cottler TG (1992) Introduction: Apoptosis in the immune system. Semin Immunol **2**: 355-362.

Hamburger V (1992) History of the discovery of neuronal death in embryos. J Neurobiol **23**: 1116-1123.

Hoffman B, Liebermann DA (1994) Molecular controls of apoptosis: Differentiation/growth arrest primary response genes, proto-oncogenes, and tumor suppressor genes as positive and negative modulators. Oncogene **9**: 1807-1812.

Humbert JR, Fermin CD, Winsor EL (1991) Early damage to granulocytes during storage. Semin Hematol **28**: 10-13.

Hyde GE, Durham D (1994) Increased deafferentation-induced cell death in chick brainstem auditory neurons following blockade of mitochondrial protein synthesis with chloramphenicol. J Neurosci **14**: 291-300.

Johnson EM, Deckwerth TL (1993) Molecular mechanisms of developmental neuronal death. Annu Rev Neurosci **16**: 31-46.

Kelley LL, Green WF, Hicks GG, Bondurant MC, Koury MJ, Ruley HE (1994) Apoptosis in erythroid progenitors deprived of erythropoietin occurs during the G1 and S phases of the cell cycle without growth arrest or stabilization of wild-type p53. Mol Cell Biol **14**: 4183-4192.

Kerr JFR, Wyllie AH, Currie AR (1972) Apoptosis: A basic biological phenomenon with wide-ranging implications in tissue kinetics. Br J Cancer **26**: 239-257.

Lassmann H, Bancher C, Breitschopf H, Wegiel J, Bobinski M, Jellinger K, Wisniewski HM (1995) Cell death in Alzheimer's disease evaluated by DNA fragmentation in situ. Acta Neuropathol **89**: 35-41.

Laurent-Crawford AG, Krust B, Muller S, Riviere Y, Rey-Cuille MA, Bechet JM, Montagnier L, Hovanessian AG (1991) The cytopathic effect of HIV is associated with apoptosis. Virology **185**: 829-39.

Lewis DE, Ng Tang DS, Adu-Oppong A, Schober W, Rodgers JR (1994) Anergy and Apoptosis in CD8+ T cells from HIV-infected persons. J Immunol **153**: 412-420.

Lu YY, Koga Y, Tanaka K, Sasaki M, Kimura G, Nomoto K (1994) Apoptosis induced in CD4+ cells expressing gp160 of human immunodeficiency virus type 1. J Virol **68**: 390-399.

McCloskey TW, Oyaizu N, Coronesi M, Pahwa S (1994) Use of a flow cytometric assay to quantitate apoptosis in human lymphocytes. Clin Immunol Immunopathol **71**: 14-18.

Motyka B, Griebel PJ, Reynolds JD (1993) Agents that activate protein kinase-C rescue sheep ileal peyer's patch B-Cells from apoptosis. Eur J Immunol **23**: 1314-1321.

Murphy K, Heimburger A, Loh D (1990) Induction by antigen of intrathymic apoptosis of CD4+, CD8+ TCR1 thymocytes *in vivo*. Science **250**: 1720-1723.

Oberhammer F, Fritsch G, Schmeid M, Printz D, Purchio T, Lassmann H, Schulte-Hermann R (1993) Condensation of the chromatin at the membrane of an apoptotic nucleus is not associated with activation of an endonuclease. J Cell Sci **104**: 317-326.

Ohno K, Okamoto Y, Miyazawa T, Mikami T, Watari T, Goitsuka R, Tsujimoto H, Hasegawa A (1994) Induction of apoptosis in a T lymphoblastoid cell line infected with feline immunodeficiency virus. Arch Virol **135**: 153-158.

Omerod MG, Sun X, Brown D, Snowden RT, Cohen GM (1993) Quantification of apoptosis and necrosis by flow cytometry. Acta Oncol **32**: 417-424.

Oppenheim RW (1984) Cell death of motoneurons in the chick embryo spinal cord. VIII. Motoneurons prevented from dying in the embryo persist after hatching. Dev Biol **101**: 35-39.

Oppenheim RW (1991) Cell death during development of the nervous system. Annu Rev Neurosci **14**: 453-501.

Rasheed S, Gottlieb AA, Garry RF (1986) Cell killing by ultraviolet-inactivated human immunodeficiency virus. Virology **154**: 395-400.

Sellins KS, Cohen JJ (1991) Hyperthermia induces apoptosis in thymocytes. Radiat Res **126**: 85-95.

Sengelaub DR, Finlay BL (1982) Cell death in the mammalian visual system during normal development: I. Retinal ganglion cells. J Comp Neurol **204**: 311-317.

Smyth MJ, Trapani JA (1995) Granzymes: Exogenous proteinases that induce target cell apoptosis. Immunol Today **16**: 202-206.

Terai C, Kornbluth RS, Pauza CD, Richman DD, Carson DA (1991) Apoptosis as a mechanism of cell death in cultured T lymphoblasts acutely infected with HIV-1. J Clin Invest **87**: 1710-1715.

Williams GT (1991) Programmed cell death: Apoptosis and oncogenesis. Cell **65**: 1097-1098.

Yin QW, Johnson J, Prevette D, Oppenheim RW (1994) Cell death of spinal motoneurons in the chick

embryo following deafferentation: Rescue effects of tissue extracts, soluble proteins, and neurotrophic agents. J Neurosci **14**: 7629-7640.

Zamai L, Falcieri E, Zauli G, Catalki A, Vitale M (1993) Optimal detection of apoptosis by flow cytometry depends on cell morphology. Cytometry **14**: 891-897.

Ziv I, Melamed E, Nardi N, Luria D, Achiron A, Ofen D, Barzilai A (1994) Dopamine induces apoptosis-like cell death in cultured chick sympathetic neurons - A possible novel pathogenetic mechanism in Parkinson's disease. Neurosci Lett **170**: 136-140.

## Discussion with Reviewers

**P.W. Hawkes:** In **Results**, the authors mention that false colour can be useful in electron microscopy too; to prevent any misunderstanding, I suggest that they make it clear that the purpose here is very different since there is now no question of improved quantitative assessment, only the comfort and convenience of the human eye are increased.

**Authors:** We agree completely with Dr. Hawkes that the addition of pseudo-color to images in video imaging is done for aesthetic purposes only, and that the addition of false colors to a black and white negative from the electron microscope do not, in any manner or form, change the original data contained therein. On the other hand, a change in the illumination path through a color object would significantly change the saturation values of pixels seen on the screen.

**D. Dinsdale:** What stain or stains provides the best discrimination between mitotic and apoptotic chromatin?

**Authors:** In thick sections (1-2 $\mu$m) from EM preparations, the best combination is provided by a mixture of 0.2% toluidine blue (TB) and 0.1% paraphenylenediamine (PDA) dissolved in warm water. The 1-2 $\mu$m thick sections examined with the light microscope allowed high resolution analysis of chromatin below the resolution of EM. Unfortunately, this mixture only yields a differential stain if the tissue was pre-fixed with osmium tetroxide, with which the PDA reacts. The stain is very unstable, precipitates out quickly, and is thus made fresh several times daily. PDA stains most anything and it can not be removed once oxidized. Sections stained with this mixture have been saved in our laboratories for over ten years without significant changes of coloration. Non-osmicated tissues embedded in wax are usually sectioned at "thicker" intervals than those embedded in plastic or epoxies. Apoptotic cells prepared for light microscopy in wax (paraffin) or methacrylate plastic (with/without osmium) require different staining procedures that we have not worked out yet.

**D. Dinsdale:** Have the authors undermined their case for HSI by submitting such convincing colour separation in Figures 7 and 8?

**Authors:** We agree with Dr. Dinsdale that if solely considered, these figures do not emphasize the advantages of color thresholding (CT) over monochrome thresholding (MT). However, Figures 5 to 8 further highlight the advantages of color thresholding, as reviewed in Fermin and Degraw (1995), and are useful for comparing and contrasting CT and MT. The ability of CT to separate groups of pixels with different saturation values illustrated in Figure 1 and expanded in Figures 5 to 8, shows that the narrow separation of pixels' saturation that is possible from 16 million color possibilities, permits a very specific identification of structures within thresholds. It is shown that pixels with similar hue (blue in this case) may have different saturation under the same lighting condition permitting their separation from adjacent blue pixels. This is usually impossible to accomplish in MT, where a much narrower separation between adjacent pixels is generally provided by pre-chosen look-up tables with a maximum of 128 possible comparisons between adjacent pixels. Thus, with CT and a color source (Figures 5-8), as opposed to MT and black and white source (Figures 11 and 12), objects with similar hues (Figure 6) often have different saturation values (Figure 7). Consequently, dense bodies with density equal to that of chromatin (Figure 5) are readily segregated from each other.

**E. Falcieri:** When studying an apoptotic model, late phase cells are clearly distinguishable by the presence of micronuclei and/or apoptotic bodies, but generally a lot of early apoptotic stages are found. They show a progressive chromatin margination until the final formation of cap-shaped compact aggregations, which appear very electron dense and sharply separated from the diffuse chromatin areas. These features are typical of apoptosis too and are very common. I wonder if and how this technique for apoptosis quantitation could be utilized in this case.

**Authors:** It is true that any assay which quantitates apoptosis captures its measurement at merely a windowed time-point in a dynamic process. Although not illustrated, marginated chromatin was also separated from mitotic and interphase chromatin throughout the studies (please refer to Figures 5-12). We considered cells demonstrating such marginated chromatin as apoptotic in our quantitation. Thus, the utility of this technique is further enhanced over other methods by encompassing this aspect of apoptosis.